Origin and age of The Hillocks and implications for post-glacial landscape development in the upper Lake Wakatipu catchment, New Zealand

McColl, Samuel T.; Cook, Simon J.; Stahl, Timothy; Davies, Timothy R. H.

Published in:
Journal of Quaternary Science

DOI:
10.1002/jqs.3168

Publication date:
2019

Document Version
Peer reviewed version

Research paper

Title: Origin and age of The Hillocks and implications for post-glacial landscape development in the upper Lake Wakatipu catchment, New Zealand.

Running Title: Origin of The Hillocks

Samuel T. McColl*[1]. Simon J. Cook[2]. Timothy Stahl[3]. Timothy R. H. Davies[3].

[1]Geosciences Group, School of Agriculture and Environment, Massey University, New Zealand. * Corresponding Author: s.t.mccoll@massey.ac.nz

[2]Geography and Environmental Science, School of Social Sciences, University of Dundee, UK

[3]School of Earth and Environment, University of Canterbury, New Zealand

Abstract

Ambiguous landscape histories can arise from equivocal or incomplete geomorphological, sedimentological or geochronological evidence. In this study, we apply quantitative analyses to robustly assess the origin and age of a field of rounded mounds, known as 'The Hillocks'. Using clast analysis, the sediment is shown to be consistent with a landslide origin but inconsistent with other glacial sediments in the region. Cosmogenic ^{10}Be exposure age dating suggests The Hillocks formed ~8 ka. Ground-penetrating radar (GPR) reveals that the deposit rests upon deltaic foreset beds, combined with topographic data, we calculate a deposit volume of ~15-27 M m^3, consistent with the estimated volume of the proposed source area. Overall, our data support a rock avalanche origin, indicating that by 8 ka the valley was ice-free at The Hillocks location, and the level of Lake Wakatipu was lower than 340 m asl by this time. The Dart River delta shoreline was situated somewhere between The Hillocks and the present-day shoreline at that time, and has prograded at a maximum average rate of 1 m a^{-1} since ~8 ka. These findings are significant given the lack of landforms by which to constrain glacial or post-glacial landscape histories in this region of New Zealand.

Keywords

Rock avalanche, landform origin, kame, paraglacial, Lake Wakatipu

Introduction

Glacial chronologies, landscape histories, and hazard assessments must be underpinned by reliable assessment of landform origin. Glacial landforms, such as moraines, can be geomorphologically and sedimentologically similar to landforms produced by other processes such as landslides (e.g. Hewitt, 1999, 2009; Putnam et al. 2010a; Ostermann et al. 2012, Cook et al., 2013, Schleier et al., 2015), leading to possible misidentification. In New Zealand, debates over landform origin bear on broader debates about the extent to which the climates and glacier fluctuations of the Northern and Southern Hemispheres are connected (e.g. Denton et al., 1999; Schaefer et al., 2006; Schaefer et al., 2009; Winkler 2014). New Zealand glaciations are important in this context because New Zealand is one of the few landmasses within the Southern Hemisphere where a terrestrial record of glaciation is preserved (Alloway et al., 2007; Sutherland et al., 2007). However, New Zealand is also prone to slope instability as a consequence of high relief, strong seismic activity, high precipitation, and deglaciation, meaning that the Quaternary landform record comprises a complex mix of mass movement and glacial deposits (e.g. Alexander et al. 2014; Reznichenko et al. 2016). Additionally, high rates of fluvial erosion and aggradation can rapidly modify and obscure these deposits. Differentiating between these landforms is essential if researchers are to make reliable paleoenvironmental and landslide hazard assessments; robust age assessment and quantitative analyses of landform characteristics provide a means for reliable landform identification and consequent landscape interpretations.

In this study, we extend earlier work by McColl and Davies (2011) who investigated 'The Hillocks' in Otago, New Zealand (Figure 1), and argued it was produced by a rock avalanche. The Hillocks landform comprises an array of mounds that rise above the surrounding Dart River floodplain. It had formerly been assumed to be a glacial kame deposit (Kenny and Hayward, 1993), and has been used in glacial reconstructions for this region (Barrell, 2011). McColl and Davies' (2011) argument for a rock avalanche origin was based on the qualitative similarity of the deposit morphology and sedimentology to other rock avalanche deposits. Here, we apply a quantitative assessment of morphology, material properties and subsurface investigation to provide a more robust means of assessing the landform origin. In addition, we apply cosmogenic ^{10}Be surface exposure dating to assess whether or not the landform age is consistent with a Late Glacial origin as previously assumed. The findings presented here shed new light on the post-glacial landscape evolution in this part of New Zealand.

Regional setting and site description

The Hillocks is an array of rounded to irregular-shaped mounds, up to 20 m in height and 140 m in long-axis, that are situated on the floodplain of the Dart River and below the south western flank of Mount Alfred, Otago, New Zealand (Figure 1). The Dart River is a large, braided river that, along with the neighbouring Rees River, feeds into the Dart-Rees delta at the head of Lake Wakatipu at ~309 m

above sea level (Figure 1). The Dart River and its tributaries drain a mountainous section of the south-eastern Southern Alps, which has peaks in excess of 2500 m above sea level. The basement geology is the Mesozoic Haast Schist Group (Turnbull, 2000), with melange and slightly foliated volcaniclastic Caples terrane predominant in the Humboldt Mountains to the west, and higher-grade schists (textural zone IIB and IV with well-developed foliation and alteration) of the Caples and Rakaia terranes in the Barrier Range and Forbes Mountains to the north and east (Figure 1). Immediately adjacent to The Hillocks, on the western rock slope of the Dart Valley, the (textural zone IIB) semischist is replaced by the Bold Peak Formation, a dominantly-sandstone member of the Caples Terrane with textural zone IIA giving way to textural zone I (i.e. unmetamorphosed) towards the top of the rock slope (Figure 1; Turnbull, 2000). The source area for The Hillocks rock avalanche, proposed by McColl and Davies (2011) is within the Bold Peak Formation (Figure 1) at the top of the rock slope. The north-striking West Wakatipu Fault, which is likely active (Barrell, 2019), separates the Bold Peak Formation from the IIB semischist, and traverses the slope below the proposed rock avalanche source area. The potential for seismically-triggered slope failures in the region is high, with the active Alpine Fault and Nevis-Cardrona Fault, and numerous potentially active faults (including the West Wakatipu Fault) located within 60 km of The Hillocks. Stirling et al. (2012) estimate a regional probabilistic peak ground acceleration of 0.5-0.6 g over a 475-year return time, resulting in a high probability of co-seismic slope failures in

this region. At least one of the large landslides in the Dart River catchment is thought to have been co-seismically generated (Wood et al., 2011).

[Insert Figure 1]

The basin of Lake Wakatipu and the catchments that feed into it have been glaciated during the Quaternary (Turnbull, 2000; Barrell, 2011). Today, the ~6 km long Dart Glacier sits at the head of the Dart catchment, but it once would have fed a much larger glacier system that filled the Wakatipu basin during Quaternary glaciations. Lake Wakatipu, 309 m above sea level, now occupies this glacially overdeepened trough, which is ~80 km long, with a maximum depth (to lake-bed, rather than bedrock trough) of 380 m (Brodie and Irwin, 1970). At its maximum extent during the Otira Glaciation (marine isotope stages [MIS] 2-4; ~65 ka to 11.5 ka; Barrell, 2011), the glacier would have terminated at the southern end of the lake (Figure 1 C), where it deposited a suite of large terminal moraines (Barrell, 2011). These moraines are some 86 km down-valley from The Hillocks and 135 km down-valley from the present-day Dart Glacier terminus. Glacial erosional evidence and scattered glacial deposits exist high on the valley sides throughout the Wakatipu basin and, along with the Otiran terminal moraine, has allowed mapping of the maximum extent of glaciations (Barrell, 2011). However, there is sparse evidence for reconstructing the post-LGM deglaciation history of the Wakatipu basin, by contrast with other regions of New Zealand where late-Glacial and Holocene terminal positions have been identified (e.g. by moraines associated with the Antarctic Cold Reversal) (e.g. Putnam et al., 2010b).

There is evidence, represented by stranded lake shorelines, alluvial fan terracing, and delta foresets, that Lake Wakatipu has previously been up to ~50 m higher than the present day (Kober, 1999). Radiocarbon dating of wood excavated from one of the shorelines cut 26 m above the current lake level, suggests the lake was at that level at ~10 ka BP (Bell, 1992). The highest preserved shoreline (~ 50 m above modern lake level, at ~360 m asl), is suggested to have formed at least 1000 years earlier (Bell, 1992, Kober, 1999; Thomson, 1996; Sutherland et al., 2019). Other than this, little is known of the absolute timing of prehistorical lake level changes or positions of the Dart River delta. Foreset beds associated with a Lake Wakatipu delta are preserved east of Mt Alfred at an elevation of ~358 m asl (Kober, 1999), which is about 10 m above the modern Dart River floodplain at The Hillocks.

Methods

To assess the origin, history, and characteristics of The Hillocks, we use a combination of morphological, sedimentological, geophysical, and chronological tools.

Lithology and sedimentology

Samples of 50 clasts were extracted from river-cut exposures of The Hillocks sediment as well as from a range of other sediment types for use as comparisons. All clast measurements were made by a single person for methodological consistency. Comparison sites included river gravels from the

neighbouring Rees River (hereafter referred to as 'river sediment'), diamictons of glacial origin either from till exposures cut by the Rees River, or from glacial deposits reworked by debris flows at Muddy Creek (as reported in Cook et al., 2014; hereafter referred to as 'glacial sediment'), and from alluvial fan deposits close to Kinloch, ~8 km south of The Hillocks (hereafter referred to as 'alluvial fan sediment'). Following the methodology of Benn (2004), the long (a), intermediate (b) and short (c) axes of each clast were measured, as well as the roundness according to the classification scheme of Powers (1953), and facets, which would be expected in samples influenced by subglacial wear. C_{40} values (i.e. the proportion of clasts with a c:a axial ratio of ≤ 0.4, which represent more slabby and elongate shapes) were calculated for each sample, as well as the RA (relative angularity) value (i.e. the proportion of clasts in each sample that were classed as angular or very angular). Plots of C_{40} against RA have been shown to be useful in differentiating between samples of different origins, including between glacial and rock avalanche deposits (e.g. Benn and Ballantyne, 1994; Benn, 2004; Cook et al., 2013).

Age assessment

To assess the age of The Hillocks, we applied in-situ cosmogenic ^{10}Be exposure dating to boulders on mounds and other deposits assumed to be related to The Hillocks. One boulder (WP166) was sampled from a boulder accumulation below the rock avalanche source area suggested by McColl and

Davies (2011), one boulder (HB24) was sampled from the debris fan at the base of the hillslope, and two boulders (HB14 & HB20) were sampled from mounds on the valley floor (Figure 2). All samples appeared to be of similar lithology – slightly weathered, slightly foliated grey sandstone, with thin dark veins or laminations, and mm-cm thick quartz veining common, and are inferred to be part of the Bold Peak Formation. To minimise the chance of selecting boulders or boulder surfaces that would provide unrepresentative exposure ages, we applied the following sampling criteria: i) the boulders were larger than 1 m in diameter; ii) the boulders were at the higher parts of the local topography (i.e. on top of mound, fan, boulder pile) and therefore less likely to have rolled/toppled since their original emplacement; iii) the sampled surface of the boulder was more than 0.5 m above any surrounding soil; and iv) for the debris fan and floodplain, the boulders had mean Schmidt hammer (N-type) rebound values that were within the standard deviation range of all sampled boulders – rebound values were not collected from boulders near the hypothesised source area. Schmidt hammer rebound values (c.f. Goudie, 2006) were measured at least three times for each boulder, discarding the lowest measurement on each boulder. Additionally, rebound values were measured on several boulders in the Dart River to compare fresh (fluvially eroded) boulders with the weathered boulders sampled for cosmogenic dating.

Where possible, surfaces with visible, protruding quartz veins were targeted for cosmogenic sampling. A hammer and chisel were used to chip off 1-3 cm (average of 1.5 cm) thickness of rock and quartz veins from the boulder surfaces.

Topographic shielding corrections were calculated from skyline surveys at each sampling site, and boulder position and elevation measured with a Trimble GeoXH differential GPS, corrected against the Land Information New Zealand geodetic network.

Quartz was isolated following standard mineral separation procedures. Beryllium targets for two of the samples (HB20 and WP166) were prepared at University of Canterbury and, the other two (HB14 and HB24) were prepared at GNS Science and Victoria University of Wellington. The beryllium of samples and blanks was measured by the GNS Science Accelerator Mass Spectrometer. For WP166 and HB20 correction was made for a single processing blank (NZ0724) ($5.5 \pm 1.7.10^7$ a ^{10}Be; < 7%) and for HB14 and HB24 two processing blanks (KV322 and KV332) were averaged and the correction was less than 12 % ($1.8 \pm 0.3 .10^5$ a ^{10}Be). Exposure ages, using processing-blank corrected data, were calculated using the online exposure age calculator (version 3; Balco et al., 2008) using the Putnam et al. (2010a) Macaulay valley, New Zealand ^{10}Be production rate, and the time-dependent 'LSDn' scaling method. ^{10}Be ages presented in this study are not corrected for erosion; though up to ~ 1 cm of quartz vein relief on the boulders indicates that at least some surface erosion has taken place since exposure. The ages are also not corrected for snow shielding or burial by loess or soil but these potential influences were minimised by selecting protruding boulders from local topographic highs.

[Insert Figure 2 here]

Sub-surface investigation

Ground Penetrating Radar (GPR) was used to assess the internal structure and depth (i.e. total thickness) of the sediments comprising the mounds, and the nature of underlying and overlying sediments. A PULSE EKKO PRO GPR was deployed across four transects (Figure 2) toward the distal edge of the mound distribution; Transect A is 100 m long, parallel to the Dart Valley axis, and extends over a mound at the downstream end; Transect B is 100 m long, oriented perpendicular to the valley axis and crosses two mounds of low (< 5 m) relief; Transect C is 200 m long, oriented perpendicular to the valley axis, and crosses one small (< 2 m high) mound; Transect D is 150 m long, parallel to the valley axis, and crosses two mounds. For transects A, B and D, 100 MHz unshielded antennas were used; 50 MHz antennas were used for Transect C. Topographic profiles were measured using tape and laser rangefinder (Transect B) and differentially-corrected Trimble GPS (Transects A, C, and D). Radargrams were prepared using EKKO Project 3 software. An average velocity of 0.08 m/ns, as assessed by three common mid-point surveys and hyperbola velocity calibration, were applied to all radargram transects to apply topographic and depth corrections. Dewow and AGC gains were applied to enhance deeper reflectors.

Deposit volume and morphometry

The size distribution and volume of mounds comprising The Hillocks were measured to characterise the geometry of the deposit and provide a revised minimum estimate for the landform's total volume. An aerial LiDAR point cloud (of classified ground points) of the Dart River floodplain for The Hillocks area was collected and supplied by Otago Regional Council in 2019. This was converted to a 1 m resolution digital elevation model (DEM) and hillshade model. Outlines of the mounds were mapped from the hillshade model and accompanying LiDAR orthophotos. Mounds were mapped only if there was high confidence in the presence of a mound; about two-thirds of the mapped mounds were verified in the field. The deposit is partly covered by loess and alluvium, the latter indicated by the presence of paleo braid channels between mounds and fluvially-rounded gravels overlaying the angular diamicton exposed in bank sections (McColl and Davies, 2011). The depth of the alluvium (z) was estimated by ground penetrating radar (GPR). To account for this alluvial cover in measuring mound geometry, we widened the extent of the mound polygons by a constant buffer distance (w), assessed by $w = \tan\beta.z$, where β is the angle of the sides of the mounds (Figure 2). A representative slope angle for all mounds was estimated by calculating the mean pixel value of a 1 m resolution slope raster set within a 5 m buffer (5-10 m inside from the mapped mound extent) of mounds of greater than 150 m^2 (Figure 2).

A minimum (but maximum empirically-constrainable) volume of subaerial mounds was calculated by multiplying the mound area by average mound height. The buried volume of mounds beneath the alluvial cover was added to this

volume calculation by multiplying the mound area by the thickness of alluvial cover (z), with the mound area extended by (half of) the buffer width (w) to account (the wedge-shaped) volume of outer mound buried by alluvium. In calculating mound volume, we ignore any mounds removed by erosion or buried by fluvial or aeolian sediments, but consider that post-event changes in deposit morphology are unlikely to affect our volume estimate by more than ±10 %. We plotted the size frequency distribution of the mounds (volume and area). Cross-sections were also constructed to show the gross topographic profile of the mounds at directions perpendicular and parallel to the assumed rock avalanche travel direction across the valley, using a swath of random elevation points on the mounds. The remaining volume of the rock avalanche beneath the rock avalanche mounds is calculated by assessing the inferred planimetric area of the entire deposit, and multiplying by a thickness (i.e. depth to the base of the rock avalanche deposit) measured by GPR. The planimetric area was inferred to extend 50-100 m beyond the visible extent of the mounds, based on interpretation of the radargrams.

Results

Sedimentology

The Hillocks sediments are angular to very angular, clast-supported, poorly sorted, and lack bedding structures (Figure 3). The majority of the sediments are the same rock type, slightly metamorphosed sandstone similar to that found in

the proposed source area and assumed to be Bold Peak Formation. Along the northern edge of the mapped deposit, pelitic semischist clasts were present, which are similar to pelitic semischist found in-situ on the lower western slopes adjacent to The Hillocks, and inferred to be part of the IIB semischists mapped by Turnbull (2000) (Figure 1). The Hillocks sediments represent a distinct population in terms of clast shape and roundness when compared to other sediment types found in the local area (Figure 4). Whilst the range of C_{40} values of The Hillocks sediment are not dissimilar to glacial, fluvial and alluvial fan sediments, the overall average C_{40} value (60 %) is lower than other sediments in the region, and the RA value is much higher (82 % on average). The C_{40} and RA values are compatible with C_{40} and RA values measured for rockfall and other supraglacial debris found in New Zealand and globally (Figure 4); we note a difference in C_{40} values for the fluvial and glacial sediments in the Wakatipu region compared to other localities, which may relate to a difference in lithology. Facets were not found on any of The Hillocks clasts, whereas they were relatively common in the glacial (mean = 47 ± 8 %; from 6 sample sets), fluvial (mean = 24 ± 12 %; from 3 sample sets), and alluvial fan (mean = 86 ± 3 %; from 2 sample sets) facies in the region.

[Insert Figure 3 here]

[Insert Figure 4 here]

Age assessment

The boulders selected for ^{10}Be cosmogenic measurement yielded mean Schmidt hammer (SH) rebound values within the standard deviation of the SH-measured boulders from the mounds and debris fan samples (Figure 5). This provided further support, to the geomorphic criteria for sample selection, that the ^{10}Be sampled boulders were representative of The Hillocks mounds; that is to say it is unlikely that they have anomalously young (e.g. from overturning or burial) or old (e.g. from inheritance) exposure ages. The boulders in the active river channel, which are fluvially-abraded, had a significantly higher mean rebound value ($\bar{x}$ 56.5, σ4.4; T = 4.95; df = 9, p = 0.000; for a two sample, unequal variances, one-tail t-test) than on the mounds or debris fan, as expected. The mean SH value ($\bar{x}$ 44, σ5.3) for all measured mound boulders was slightly lower than the mean value ($\bar{x}$ 45.6, σ4.1) for the debris fan boulders, but not significantly higher at α=0.05 (for a two sample, unequal variances, one-tail t-test; T = 1.56; df = 15; p = 0.07).

The ^{10}Be cosmogenic measurements yielded ages (±1 σ) of 8.3 ± 0.6 and 7.6 ± 0.5 ka for the mound boulders, 7.0 ± 0.5 ka for the debris fan boulder, and 7.6 ± 0.3 ka for the source area boulder (Table 1; Figure 5). These ages are statistically indistinguishable at 95 % confidence level, according to a reduced chi-squared test (with a weighted mean and standard deviation of 7.6 ± 0.4; X_R^2 = 1.08, κ = 2.63; following equations of Jones et al. 2019). This suggests that they could represent a single event. However, as the source area boulder is on a separate landform to The Hillocks mounds and debris fan (i.e. a ridge of boulders), it is more appropriate to exclude it from an age estimate for The

Hillocks. Based on sedimentology there is no reason to treat the debris fan as different to the mounds, and a fan is expected to have been produced at the base of the slope by the same flow of material that went on to form the mounds. Nonetheless, congruent with the SH R-values, the debris fan has a younger ^{10}Be exposure age than the mounds (without overlapping of 1 σ uncertainties). The debris fan boulder is located on top of the debris fan, and while it may have originated in the same event, it is quite possible that this boulder was transported to the debris fan at a later date, some ~1 ka after the formation of the mounds; we might expect that the fan would continue to build after its initial formation. If the debris fan boulder is excluded, the two mound boulders yield a weighted mean age and standard deviation of 7.9 ± 0.4 ka (which is close to the normal kernel density, or camel diagram, estimate of 7.8 ka; Figure 5). If the debris fan sample is included it yields a weighted mean age of 7.6 ± 0.5 ka.

[Insert Table 1 here]

[Insert Figure 5 here]

Subsurface information

Radargrams for all transects reveal layers of sediment draping between the mounds, interpreted to be fluvial sediments/flood deposits associated with an abandoned braid plain (with lower boundary marked by blue line in Figure 6). The thickness of alluvium is estimated from the radargrams to be up to 4 m, but mostly around 2 m thick. A value of 2 m was used as a representative thickness (z) for calculating mound volume. Reflectors below the alluvial drape and in the

mounds are chaotic, with hyperbola tails likely indicating blocky or boulder structure, consistent with bouldery diamicton. The chaotic material generally overlies more structured, parallel, gently inclined reflectors interpreted to be bedded fluvial sediments (or topset beds) formed by migrating braid channels and bars, but in places the base is difficult to distinguish. The contact between the upper chaotic material and the lower structured material is more visible, and relatively planar, in the valley-parallel transects (Figure 6; red line on A and D) and the thickness of the chaotic material appears to be greater down valley (i.e. thicker in Transect D than in Transect A). The contact is more difficult to discern in the valley-perpendicular transects (Figure 6; red line on B and C), and is more undulating and possibly stepping down towards the west / valley-centreline (Figure 6; red line on C), suggesting terraces. The thickness of the chaotic material is estimated to be between 4 to 12 m. In Transects A and D, which are parallel to the valley axis, more steeply inclined, parallel reflectors (orange lines in Figure 6) dip down-valley and are interpreted as deltaic foreset beds of a prograded delta (with upper contact with topset or other alluvium represented by orange line in Figure 6).

[Insert Figure 6 here]

Deposit volume and morphology

The volume of material occupied by the 169 mapped mounds is calculated to be 1.6 M m^3. The area of the entire mapped deposit is calculated as 2 M m^2, and using the 4-12 m range of thickness estimated by GPR, suggests a further 8 to

24 M m^3 is buried beneath the floodplain alluvium, giving a total deposit volume likely between ~10 and 26 M m^3. The deposit is dominated by mounds with areas between 500-2000 m^2 and volumes between 1000-5000 m^3, with smaller mounds (according to area, volume and height; Figure 7 A, B, and D respectively) towards the east. The gross morphology of The Hillocks appears to thin outwards towards the edges in the transverse swath (Figure 7C), but with the highest mound features not at the centre of the transect due to two large mounds at 350 m and 950 m from the section origin (Figure 7C). In an across-valley direction (longitudinal relative to hypothesised rock avalanche travel direction; Figure 7D), the mounds are at their highest at about 550 m from the origin, and reduce in height gradually across valley to the east, and decline more sharply towards the west (Figure 7D). The base of The Hillocks gradually rises towards the east (from about the 600 m distance mark on Figure 7D).

[Insert Figure 7 here]

Discussion

Origin of The Hillocks

Our results support the conclusion of earlier work by McColl and Davies (2011) who had suggested a landslide origin for The Hillocks. Sedimentological data confirm that The Hillocks debris is angular and mostly monolithic, is poorly sorted and lacks bedding structures (i.e. is a diamicton; Figure 3). These

characteristics are consistent with other observations of rock avalanche sedimentology (e.g. Hewitt, 1999, 2009; Dufresne et al., 2016; Cook et al., 2013; Dunning, 2006), but different from glacially derived sediments in the region (Figure 4). The morphology and presence of mounds making up The Hillocks are also consistent with rock avalanche deposits (Dufresne and Davies, 2009). McColl and Davies (2011) observed a crudely radial alignment of mounds spreading out from the western valley side. The morphometric analyses in this study (Figure 7 C & D) support this, demonstrating a lowering of mound height towards the east (i.e. distal from source) and a lowering of heights on the lateral margins of the deposit, which is consistent with a rock avalanche spreading and thinning out over a relatively unconfined surface (Dufresne, 2009; Paguican et al., 2014); we note that there may have been some terracing of the substrate representing several metres of relief across the valley floor (Figure 6C). The reduction in mound size (Figure 7 A & B) with travel distance is also common for avalanche deposits (Paguican et al., 2014), but there is no obvious reason why a glacier would create such a notable cross-valley distribution of mound sizes. Further, the geochronological data presented here indicate that The Hillocks was deposited at ~7.9 ka. An earlier compilation of mapped landforms by Barrell (2011) was used to reconstruct a series of ice limits for the Wakatipu Glacier; a Late MIS2 (18-30 ka) ice margin, incorporating The Hillocks, was drawn for the Dart valley. The cosmogenic dating presented here indicates that The Hillocks formed after the Late Glacial, and certainly after MIS2. We suggest that the glacier terminus would likely have retreated beyond The Hillocks well before 7.9

ka for two reasons: i) geological evidence (e.g. Kober, 1999) and topographic profiling suggest that the lake would have extended farther up valley than The Hillocks, making a stable terminal position at or downstream of The Hillocks unlikely; and ii) the Dart River must have subsequently prograded downstream of The Hillocks prior to their formation, as supported by the observation in the radargrams (Figure 6) of deltaic foreset beds underlying the diamicton. There is also no evidence (c.f. Ballantyne, 2018) of a glacial readvance over The Hillocks, which could have reset exposure ages; although it is recognised that a thin glacier over a short duration may not cause an obvious modification (Cook et al., 2013). Moreover, glacial chronologies from other eastern South Island glacial valleys (e.g. Putnam et al., 2010b; Kaplan et al., 2013) have shown that by about 8 ka glacier limits were closer to their Little Ice Age and present-day limits than their late Glacial (i.e. Antarctic Cold Reversal; 14.5-12.7 ka) limits, indicating relatively small Holocene glaciers. The Hillocks is almost 50 km down valley of the present-day Dart Glacier terminus, so by 8 ka the terminus is likely to have been much farther up valley than The Hillocks. Taken together, it is difficult to reconcile the observations in this study and McColl and Davies (2011) with the long-held view that The Hillocks represent a glacial deposit (Kenny and Hayward, 1993). The evidence presented in this study is consistent with a rock avalanche origin for The Hillocks.

Rock avalanche volume and source

Using GPR and new topographic data, the volume of The Hillocks deposit is estimated to be within a range of 10 to 26 M m^3. To estimate the total rock avalanche deposit volume, we round these values up to 11-27 M m^3 to conservatively account for an unquantified amount of material deposited at the base of the source area and possibly along the transport path. This range fits with the 22.5 M m^3 volume estimated for the source area hypothesised by McColl and Davies (2011), who had identified a basin at the top of the western hillslope (Figure 8). The lithology of the rocks found in the source area also appears similar to the sediments in The Hillocks and debris fan. A rock type, of minor overall constituent, was found within a mound on the northern edge of The Hillocks and appears to be the same as a band of in-situ bedrock (pelitic semischist of textural zone IIB; Figure 1) observed near the base of the valley slope. This suggests there must have been at least some additional entrainment of material by the rock avalanche. Overall, we provide further support for the source area proposed by McColl and Davies (2011). While not entirely convincing in form as a landslide source area, rockfall and other erosion over the past 8 ka would have modified this basin considerably, explaining why today it poorly resembles a landslide scar.

[Insert Figure 8 here]

Implications for landscape development chronology

The identification of The Hillocks as a landslide deposit has implications for understanding glacial and post-glacial landscape change in the Wakatipu region. Landforms of glacial deposition are sparse in the Wakatipu region (Barrell, 2011), and very few deposits of any origin have been dated. Our results indicate that The Hillocks deposit cannot be used to directly reconstruct former glacier extent in the region, but its presence demonstrates that the glacier terminus was farther up the Dart valley by ~8 ka, and probably much closer to the present day Dart Glacier terminus, consistent with other glacial reconstructions from the eastern Southern Alps (Putnam et al., 2010b; Kaplan et al., 2013). Radiocarbon dating of wood fragments unearthed in lake sediments near Queenstown and Frankton demonstrate that Lake Wakatipu had begun forming (i.e. the glacier terminus had retreated past Queenstown) by at least ~10 ka BP (Bell, 1992). Taken together with data presented in this study, the position of the ice front can be constrained as having been north of Queenstown/Frankton by ~11 ka BP to somewhere likely well north (up valley) of The Hillocks by ~8 ka. Further geochronological data are clearly desirable to better constrain ice positions, but this is challenging given the lack of glacial deposits and other target landforms.

The age and position of The Hillocks also provides some constraint on the prehistoric timing and positions of the Dart River delta and the level of Lake Wakatipu. It is inferred that the delta foreset beds preserved on the eastern side of Mt Alfred, which outcrop there some 10 m above the modern Dart floodplain, predate The Hillocks. Otherwise The Hillocks would have been underwater, which is precluded by the observation that they were emplaced onto a braid plain

and deltaic forest beds. This requires that the level of Lake Wakatipu had already dropped from its high-stand of approximately 360 m asl to lower than 340 m asl by 7.9 ka as indicated by the elevation of the foreset beds underneath The Hillocks deposit (Figure 6), so that it was between 340 m asl and the present level of 309 m asl. This is consistent with Bell (1992) whose dating suggests a lake level of 335 m asl (26 m above present level) by ~ 10 ka. The Dart River delta (i.e. lake shoreline) therefore must also have been some distance downstream by this time; the modern delta is ~8 km from the downstream edge of The Hillocks. This provides a constraint on the maximum delta progradation rates, of 1 km ka^{-1} (1 m a^{-1}) on average since ~ 8 ka. Historical rates of progradation of the Rees-Dart delta, assessed from historical aerial photo interpretation by Wild (2013), are 1.7 m a^{-1} from 1966 to 2007 (averaged from an aerial increase of 203,000 m^2 over a delta width of 2850 m). Likewise, modelled average progradation over the next 120 years is 1.4 m a^{-1}, with a range of between 0.4 and 2.5 m a^{-1} (Wild, 2013). These historical and projected rates are higher than the maximum rate estimated since 8 ka. This discrepancy suggests that either by 8 ka the delta shoreline was relatively close to The Hillocks, and/or that historical sediment supply is higher than during the Holocene (possibly increasing once Rees River coalesced with Dart River) or geometrical changes (e.g. lake depth) have resulted in faster progradation.

We observed up to 4 m of fluvial sediments draped between the hummocky topography of The Hillocks, so the Dart River has occupied a surface (5-6 m) higher than its modern channel since the emplacement of The Hillocks. The

topographic profiling (Figure 7 D) and the pattern of braid plain channels (Figure 2) suggest paleo channels flowed towards the south-west across The Hillocks from the north-eastern edge of the deposit (an area of low, small mounds). Subsequent headward incision between, or connection through, some of the larger mounds on the west may have eventually allowed a channel avulsion to produce the present configuration, which appears today to be stable, and with The Hillocks constricting the river at this point. The elevated alluvial surface may relate to aggradation associated with delta progradation and its abandonment may relate to continued lowering of the level of Lake Wakatipu. Wild (2013) noted that aggradation-degradation phases may be a characteristic of the Dart River floodplain, and this may also explain our observation of terraces (i.e. incision) at the base of the rock avalanche (Figure 6 C). Alternatively, the surface and its abandonment may relate to a blockage of the Dart River by the rock avalanche, possibly driving temporary ponding and aggradation upstream, overtopping, and eventual breaching following channel avulsion through the larger mounds to the west.

McColl and Davies (2011) suggested that The Hillocks may be a coseismic landslide deposit based on the observation of a deep-seated source area at the top of a steep slope, consistent with observations made following other coseismic landslide events (McSaveney et al., 2000); by contrast, historical aseismic events in New Zealand more often involve the failure of a spur or slab of rock (e.g. Owens, 1992; Hancox et al., 2005). If a seismic event did trigger The Hillocks landslide at ~8 ka, it may have triggered other landslides in the region. Sweeney

et al. (2013) dated the Lochnagar landslide deposit, ~30 km northeast from The Hillocks, to between 6.3 ± 0.3 to 8.9 ± 0.5 ka, favouring an older age within this bracket. The authors did not specify a triggering mechanism, but suggested a seismic event could have initiated the failure. Thus, in addition to future work on dating glacial landforms, it would be valuable to date other pre-historic landslide deposits in the region (e.g. those farther up the Dart River; Cox et al., 2014) in order to determine whether there is a broader evidence base for a major earthquake at this time.

Conclusions

Information on landform morphometry, sedimentology, and age presented in this study favour a rock avalanche origin for The Hillocks in Otago, New Zealand. Clast morphologies within The Hillocks deposit are consistent with rock avalanche deposits, but not with other proposed deposits or mechanisms. The morphology and distribution of the mounds suggests thinning of the deposit, and reduction in mound size in a cross-valley direction away from the proposed source area. The most plausible source area identified for the landslide seems to be the basin to the west, which has a scar with a volume compatible with the volume measured for The Hillocks, and has produced boulders with a lithology matching that of The Hillocks. GPR data indicate that the deposit was emplaced upon a braid plain and prograded delta. ^{10}Be exposure-ages of ~ 7.9 ka for the mounds, and statistically-indistinguishable ages for adjacent landforms assumed

to be related, provide further support for a rock avalanche origin, and indicate a Holocene timing for that event. These new data show that by 7.9 ka the former Wakatipu Glacier had certainly retreated up valley past this location, and Dart River had prograded down valley of this location, providing useful constraints on glacial and post-glacial chronologies in the otherwise fragmentary record of events in this catchment. Furthermore, this study demonstrates the utility of quantitative methods of landform identification and analysis for informing studies that utilise landforms for paleoclimate or landscape reconstructions.

Acknowledgements

We thank Duncan Quincey, Emma Cody, and Florian Strohmaier for assistance in the field; Otago Regional Council for supplying LiDAR data; Sacha Baldwin and Gregory De Pascal for assistance with cosmogenic sample preparation; and the land custodians for access to the field site. SJC acknowledges funding from the Aberystwyth University Research Fund, STM acknowledges funding from Massey University (RM17927). Much of the analysis and writing of this manuscript was undertaken whilst SJC was in receipt of a Massey University Visiting Scholarship and STM in receipt of a University of Dundee ISSR Global Scholar grant. We are grateful to the three reviewers who provided thoughtful suggestions which helped us to improve this manuscript.

References

Alexander, D., Davies, T., Shulmeister, J., 2014. Formation of the Waiho Loop terminal moraine, New Zealand. Journal of Quaternary Science, 29(4), 361-369.

Alloway, B.V., Lowe, D.J., Barrell, D.J., et al., 2007. Towards a climate event stratigraphy for New Zealand over the past 30 000 years (NZ-INTIMATE project). Journal of Quaternary Science, 22(1), 9-35.

Balco, G., Stone, J.O., Lifton, N.A., et al., 2008. A complete and easily accessible means of calculating surface exposure ages or erosion rates from 10Be and 26Al measurements. Quaternary Geochronology, 3(3), 174-195.

Ballantyne, C.K., 2018. Glacially moulded landslide runout debris in the Scottish Highlands. Scottish Geographical Journal, 134(3-4), 224-236.

Barrell, D.J.A., 2011. Quaternary glaciers of New Zealand. In: J. Ehlers, P.L. Gibbard, P.D. Hughes (Eds.), Developments in Quaternary Science, 15, 1047-1064. Elsevier.

Barrell, D.J.A. 2019. General distribution and characteristics of active faults and folds in the Queenstown Lakes and Central Otago districts, Otago. Lower Hutt (NZ): GNS Science. Consultancy Report 2018/207.

Bell, D.H., 1992. Geomorphic evolution of a valley system: The Kawarau Valley, Central Otago. In: J.M. Soons, M.J. Selby (Eds.), Landforms of New Zealand. Longman, Auckland, pp. 456-481.

Benn, D.I., Ballantyne, C.K., 1994. Reconstructing the transport history of glacigenic sediments: a new approach based on the co-variance of clast form indices. Sedimentary Geology, 91(1-4), 215-227.

Benn, D.I., 2004. Clast morphology. In: Evans, D.J.A., Benn, D.I. (Eds.), A Practical Guide to the Study of Glacial Sediments. Arnold, London.

Brodie, J.W., Irwin, J., 1970. Morphology and sedimentation in Lake Wakatipu, New Zealand. New Zealand Journal of Marine & Freshwater Research, 4(4), 479-496.

Brook, M., Lukas, S., 2012. A revised approach to discriminating sediment transport histories in glacigenic sediments in a temperate alpine environment: a case study from Fox Glacier, New Zealand. Earth Surface Processes and Landforms, 37(8), 895-900.

Cook, S.J., Porter, P.R., Bendall, C.A., 2013. Geomorphological consequences of a glacier advance across a paraglacial rock avalanche deposit. Geomorphology, 189, 109-120.

Cook, S.J., Quincey, D.J., Brasington, J., 2014. Geomorphology of the Rees Valley, Otago, New Zealand. Journal of Maps, 10(1), 136-150.

Corominas, J., 1996. The angle of reach as a mobility index for small and large landslides. Canadian Geotechnical Journal, 33(2), 260-271.

Cox, S.C., Rattenbury, M.S., McSaveney, et al., 2014. Activity of the Landslide Te Horo and Te Koroka Fan, Dart River, New Zealand During January 2014. GNS Science Report 2014/07, 45 pp.

Denton, G.H., Heusser, C., Lowell, T., et al., 1999. Interhemispheric linkage of paleoclimate during the last glaciation. Geografiska Annaler: Series A, Physical Geography, 81(2), 107-153.

Dufresne, A., 2009. Influence of runout path material on rock and debris avalanche mobility: field evidence and analogue modelling. Doctor of Philosophy PhD Thesis, University of Canterbury, Christchurch, 268 pp.

Dufresne, A., Davies, T.R., 2009. Longitudinal ridges in mass movement deposits. Geomorphology 105(3-4), 171–181.

620 Dufresne, A., Bösmeier, A., Prager, C., 2016. Sedimentology of rock avalanche
621 deposits–case study and review. Earth-Science Reviews, 163, 234-259.

622 Dunning, S., 2006. The grain size distribution of rock-avalanche deposits in
623 valley-confined settings. Italian Journal of Engineering Geology and
624 Environment, 1, 117-121.

625 Goudie, A.S., 2006. The Schmidt Hammer in geomorphological research.
626 Progress in Physical Geography, 30(6), 703-718.

627 Hancox, G.T., McSaveney, M.J., Manville, V.R., et al., 2005. The October 1999
628 Mt Adams rock avalanche and subsequent landslide dam-break flood and
629 effects in Poerua River, Westland, New Zealand. New Zealand Journal of
630 Geology and Geophysics, 48(4), 683-705.

631 Hewitt, K., 1999. Quaternary moraines vs catastrophic rock avalanches in the
632 Karakoram Himalaya, Northern Pakistan. Quaternary Research, 51(3), 220-
633 237.

634 Hewitt, K., 2009. Catastrophic rock slope failures and late Quaternary
635 developments in the Nanga Parbat-Haramosh Massif, Upper Indus basin,
636 northern Pakistan. Quaternary Science Reviews, 28(11-12), 1055-1069.

637 Jones, R.S., Small, D., Cahill, N., et al., 2019. iceTEA: Tools for plotting and
638 analysing cosmogenic-nuclide surface-exposure data from former ice
639 margins. Quaternary Geochronology, *51*, 72-86.

640 Kaplan, M.R., Schaefer, J.M., Denton, G.H., et al., 2013. The anatomy of long-
641 term warming since 15 ka in New Zealand based on net glacier snowline
642 rise. Geology, 41(8), 887-890.

643 Kenny, J.A., Hayward, B.W., 1993. Inventory of Important Geological Sites and
644 Landforms in the Otago Region. Geological Society of New Zealand
645 Miscellaneous Publication, 77.

Kober, F., 1999. Late Quaternary Geology of Glenorchy District, Upper Lake Wakatipu. Postgraduate Diploma of Science of Geology Thesis, University of Otago, Dunedin, 121 pp.

Lukas, S., Benn, D.I., Boston, C.M., et al., 2013. Clast shape analysis and clast transport paths in glacial environments: A critical review of methods and the role of lithology. Earth-Science Reviews, 121, 96-116.

McColl, S.T., Davies, T.R., 2011. Evidence for a rock-avalanche origin for `The Hillocks' "moraine", Otago, New Zealand. Geomorphology, 127(3-4), 216-224.

McSaveney, M.J., Davies, T.R., Hodgson, K.A., 2000. A contrast in deposit style and process between large and small rock avalanches. In: E. Bromhead, N. Dixon, M.L. Ibsen (Eds.), VIII ISL Cardiff, Landslides in research, theory and practice. Landslides. Thomas Telford, London, 1053-1058 pp.

Ostermann, M., Sanders, D., Ivy-Ochs, S., et. al., 2012. Early Holocene (8.6 ka) rock avalanche deposits, Obernberg valley (Eastern Alps): Landform interpretation and kinematics of rapid mass movement. Geomorphology, 171, 83-93.

Owens, I.F., 1992. A note on the Mount Cook Rock Avalanche of 14 December 1991. New Zealand Geographer, 48(2), 74-78.

Paguican, E., de Vries, B.v.W., Lagmay, A., 2014. Hummocks: how they form and how they evolve in rockslide-debris avalanches. Landslides, 11(1), 67-80.

Powers, M.C., 1953. A new roundness scale for sedimentary particles. Journal of Sedimentary Research, *23*(2), 117-119.

Putnam, A.E., Schaefer, J.M., Barrell, D.J.A., et al., 2010a. In situ cosmogenic 10Be production-rate calibration from the Southern Alps, New Zealand. Quaternary Geochronology, 5(4), 392-409.

Putnam, A.E., Denton, G.H., Schaefer, et al., 2010b. Glacier advance in southern middle-latitudes during the Antarctic Cold Reversal. Nature Geoscience, 3(10), 700-704.

Reznichenko, N.V., Davies, T.R., Winkler, S., 2016. Revised palaeoclimatic significance of Mueller Glacier moraines, Southern Alps, New Zealand. Earth Surface Processes and Landforms, 41(2), 196-207.

Schaefer, J.M., Denton, G.H., Barrell, D.J.A., et al., 2006. Near-synchronous interhemispheric termination of the Last Glacial Maximum in mid-latitudes. Science, 312(5779), 1510-1513.

Schaefer, J.M., Denton, G.H., Kaplan, M., et al., 2009. High-Frequency Holocene Glacier Fluctuations in New Zealand Differ from the Northern Signature. Science, 324(5927), 622-625.

Schleier, M., Hermanns, R.L., Rohn, J. e.t. al., 2015. Diagnostic characteristics and paleodynamics of supraglacial rock avalanches, Innerdalen, Western Norway. Geomorphology, 245, 23-39.

Stirling, M., McVerry, G., Gerstenberger, M., et al., 2012. National seismic hazard model for New Zealand: 2010 update. Bulletin of the Seismological Society of America, 102(4), 1514-1542.

Sutherland, R., Kim, K., Zondervan, A., et al., 2007. Orbital forcing of mid-latitude Southern Hemisphere glaciation since 100 ka inferred from cosmogenic nuclide ages of moraine boulders from the Cascade Plateau, southwest New Zealand. Geological Society of America Bulletin, 119(3-4), 443-451.

Sutherland, J.L., Carrivick, J.L., Shulmeister, J., et al., 2019. Ice-contact proglacial lakes associated with the Last Glacial Maximum across the Southern Alps, New Zealand. Quaternary Science Reviews, 213, 67-92.

Sweeney, C.G., Brideau, M.A., Augustinus, P.C., et al., 2013. Lochnagar landslide-dam – Central Otago, New Zealand: Geomechanics and timing of the event, In C.Y Chin (Ed.), 19th New Zealand Geotechnical Society 2013 Symposium: Hanging by a thread?: lifelines, infrastructure and natural disasters, Queenstown, November 2013. Wellington, NZ: Institute of Professional Engineers New Zealand. Proceedings of technical groups (Institution of Professional Engineers New Zealand).

Thomson, R., 1996. Prehistoric changes in the level of Lake Wakatipu. An unpublished outline study prepared for the Otago Regional Council, 4 pp.

Turnbull, I.M., 2000 (compiler). Geology of the Wakatipu area, Institute of Geological and Nuclear Sciences 1:250 000 geological map 18. Institute of Geological and Nuclear Sciences Limited, Lower Hutt, New Zealand. Map (1 sheet) + 72 pp.

Wild, M.A., 2013. Growth dynamics of braided gravel-bed river deltas in New Zealand. PhD Thesis, University of Canterbury, Christchurch, 246 pp.

Winkler, S., 2014. Investigation of late-Holocene moraines in the western Southern Alps, New Zealand, applying Schmidt-hammer exposure-age dating. The Holocene, 24(1), 48-66.

Wood, J.R., Wilmshurst, J.M. & Rawlence, N.J. 2011. Radiocarbon-dated faunal remains correlate very large rock avalanche deposit with prehistoric Alpine fault rupture. New Zealand Journal of Geology and Geophysics, 54**,** 431-434.

720 **Table 1:** Cosmogenic ^{10}Be exposure age measurements and parameters.

Sample name	Feature / location	Latitude	Longitude	Elevation (m asl)	Thickness (cm)	Density (g cm^{-1})	Shielding correction	Be-10 atoms g^{-1}	Be AMS standard	Age ± 1 σ (ka) (external error in brackets)
WP166	Near source	-44.78	168.30	1400	1.5	2.7	0.871	87194 ± 3337	NIST_27900	7.55 ± 0.29 (0.31)
HB20	Mound	-44.77	168.33	352	1.5	2.7	0.988	40031 ± 2600	NIST_27900	7.55 ± 0.49 (0.51)
HB14	Mound	-44.77	168.33	345	1.5	2.7	0.987	43977 ± 2878	07KNSTD	8.32 ± 0.55 (0.56)
HB24	Debris fan	-44.77	168.32	350	1.5	2.7	0.975	36649 ± 2372	07KNSTD	7.04 ± 0.46 (0.47)

721

722

723 **Figures:**

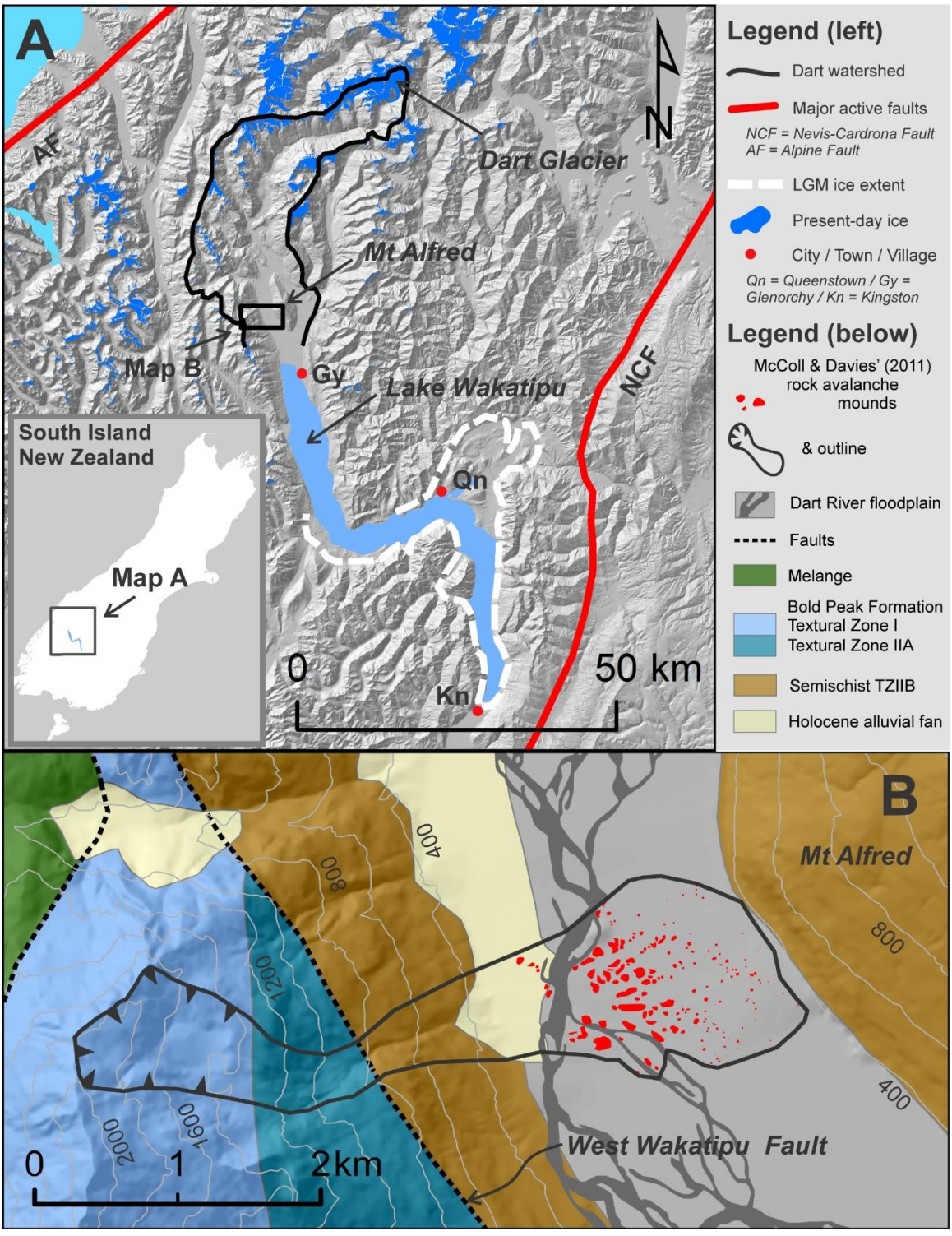

724

725 **Figure. 1:** Regional setting and site details of The Hillocks: Map A)

726 Topography of the Lake Wakatipu basin and surrounding topography, showing

727 the Dart River catchment, major active faults, modern and former ice extents and
728 present-day Dart Glacier; see inset map for location within New Zealand's South
729 Island. Map B) The Hillocks Rock Avalanche outline and distribution of mounds
730 (according to McColl and Davies, 2011), with general topography and major rock
731 types and faults shown (from Turnbull, 2000).

732

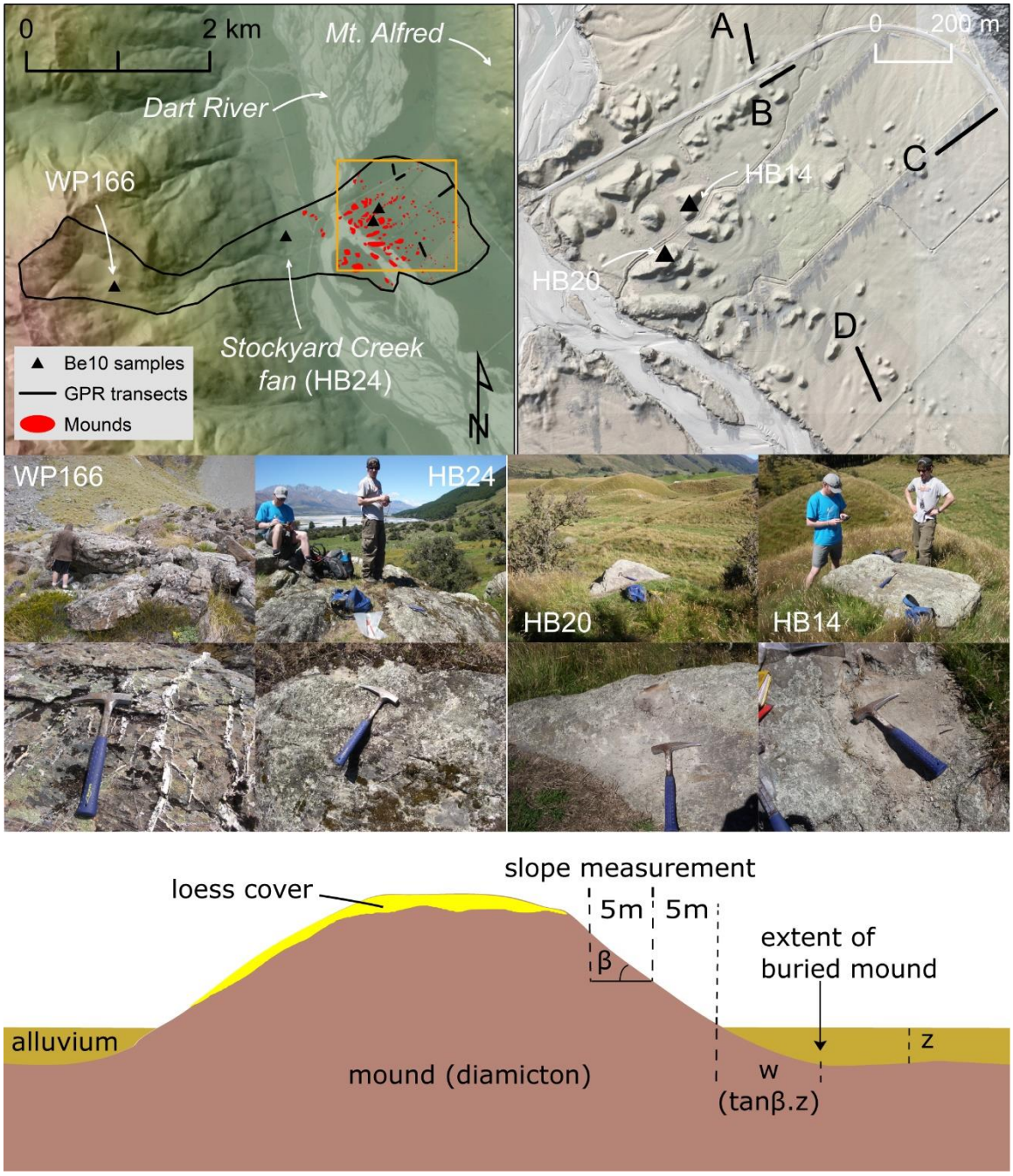

733

734 **Figure 2.** Maps showing the positioning of GPR transects and ^{10}Be
735 cosmogenic exposure age dating sampling locations. Left-hand map shows
736 outline of the rock avalanche (black outline) and mounds (red polygons) as
737 mapped by McColl and Davies (2011). A transparent LINZ 8 m DEM hillshade
738 behind an aerial image provides an impression of topographic relief. The right-

hand map shows the mounds on the floodplain, with a LiDAR hillshade model. The photos show the ^{10}Be cosmogenic sample sites and sampled boulders. The conceptual diagram below demonstrates how the extents of partially buried mounds were approximated.

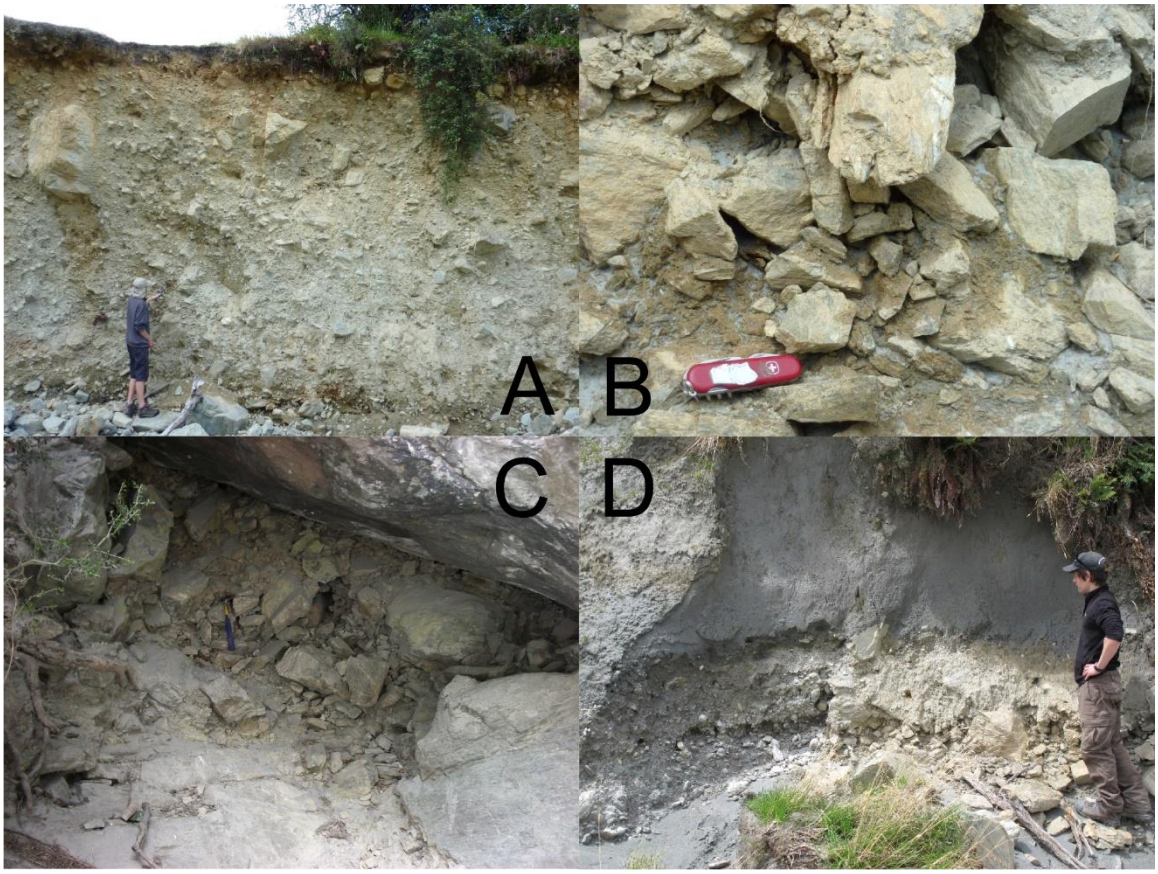

Figure 3: Sediments from exposures at The Hillocks: A) Streambank of the Stockyard Creek as it dissects the debris fan, with a notable lack of bedding, suggesting rapid emplacement possibly by the rock avalanche; B) Close up of rock avalanche sediments showing angular nature; C) Exposure of rock avalanche sediments with large boulder on top; boulder-carapaces are common

in rock avalanche deposits; D) Exposure of a mound at the Dart River with rock avalanche sediments on right (near person's legs) and coarse fluvial gravels on left, with fines (loess and / overbank silts) on top.

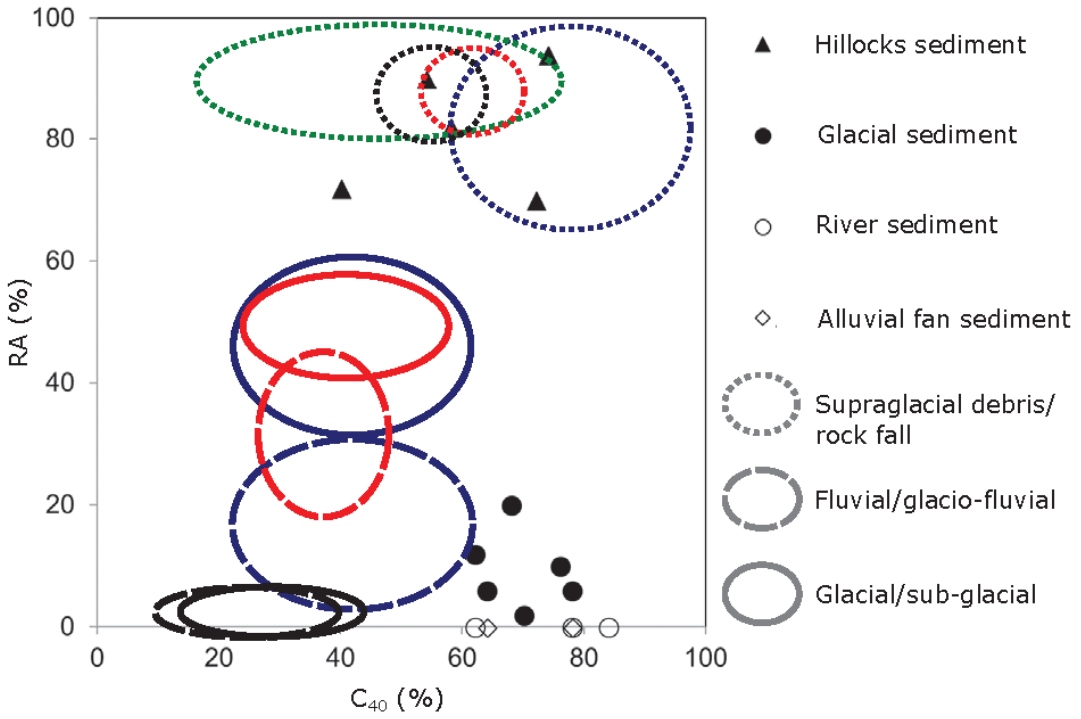

Figure 4: C_{40}-RA plot of clast data collected from The Hillocks and a range of other comparison sediment types. The RA axis represents the percentage of clasts that are angular and very angular; the C_{40} axis represents the proportion of clasts with a c:a axial ratio of ≤ 0.4 (i.e. more slabby and elongate shapes). The ellipses represent envelopes for characteristic sediment types; blue envelopes from Lukas et al. (2013) for high-mountain glaciers worldwide; red and black envelopes from Brook and Lukas (2012) for Fox Glacier, New Zealand, for schist

762 and greywacke respectively; green envelope from Reznichenko et al. (2016) for a
763 rock-avalanche dominated moraine at Mueller Moraine, New Zealand.

764

765

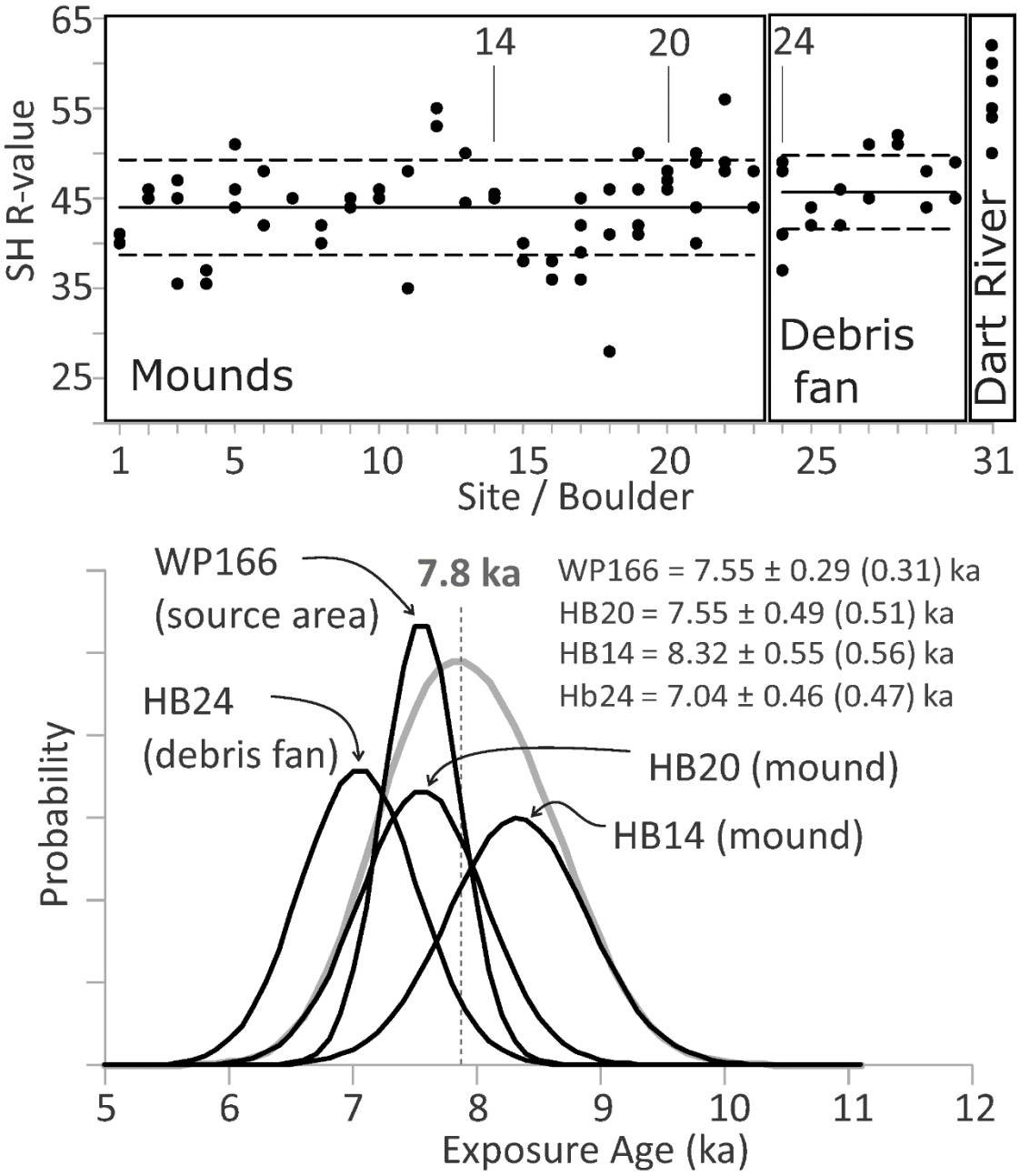

766

767 **Figure 5.** Top) Schmidt hammer rebound values for boulders on the
768 floodplain mounds, debris fan, and within the Dart River channel. Dots represent
769 single R-values. Boxes distinguish different sampling location. The Dart River
770 (31) represents aggregated values for several boulders within the channel,

whereas the floodplain and debris fan sites (i.e. boulders 1-30) have values shown for individual boulders. Solid lines show the mean value and dashed lines are ±1 σ, for the floodplain and debris fan separately. Arrows indicate boulders used for cosmogenic sampling. Bottom) ^{10}Be exposure ages and their probability density functions. Individual ages (black) are plotted as probability density functions (PDF) of a normal distribution using the measured exposure age and the (1 σ) external (i.e. measurement + production rate) uncertainty. The grey line shows the sum of the individual PDFs for the two mound samples. The peak of the summed PDF plot (solid line) presents a clustered age of 7.8 ka.

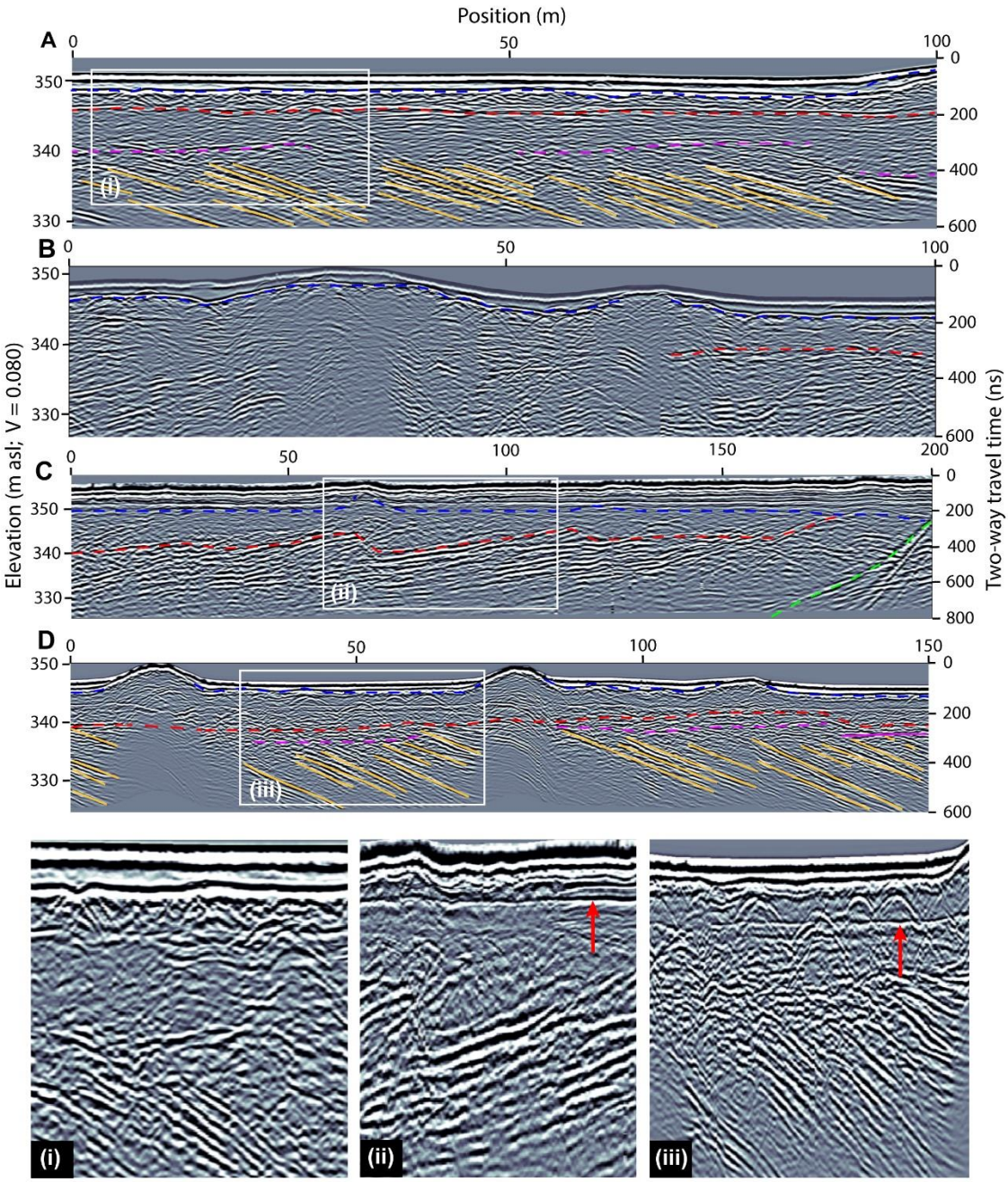

782

783 **Figure 6**: Radargrams from Transects A-D, with zoomed sections shown in
784 panels i-iii. The locations are found in Figure 2, with the beginning position (left-
785 hand side) of each transect shown by the position of the letter labels in Figure 2.
786 Representative annotations are as follows: Blue dashed line = base of alluvial fill;

Red dashed line = base of chaotic/diamicton-like material; Orange line = foreset beds; Purple dashed line = angular contact between foreset beds and overlaying alluvium; Green dashed line; top of colluvium/bedrock of Mt Alfred; Red arrows show reflector interpreted to be water table. The zoomed in panels i-iii have vertical exaggeration, whereas panels A-D have approximately equal distance-depth scales.

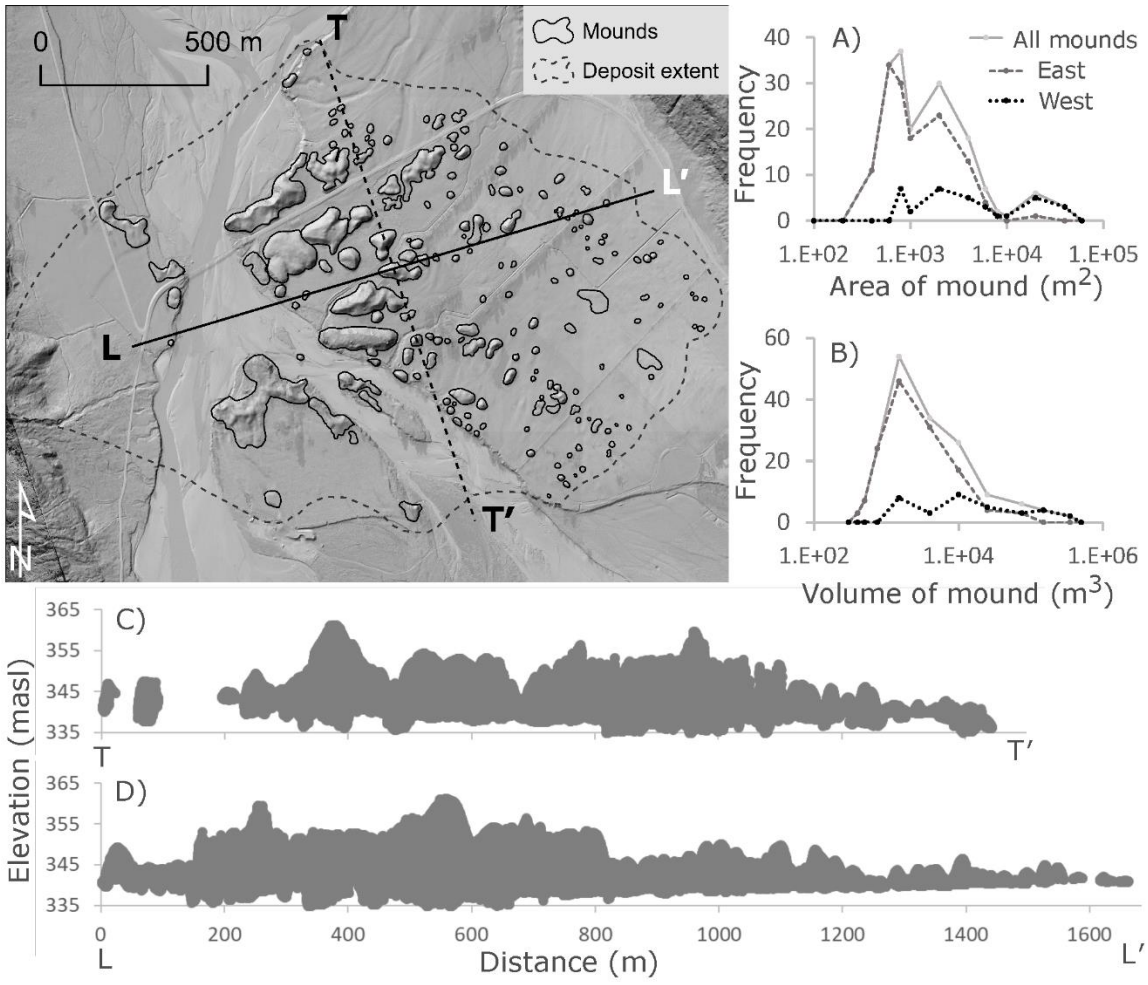

Figure 7: Area (A) and volume (B) frequency distribution curves are shown for all mounds (and also divided into mounds east and west of line T-T′ on inset map). Point elevation swath plots of the mounds are shown in transverse (C) and longitudinal (D) directions relative to hypothesised avalanche travel direction; inset map shows centreline of the transverse (T-T′) and longitudinal (L-L′) swaths, and the distribution of mounds updated in this study.

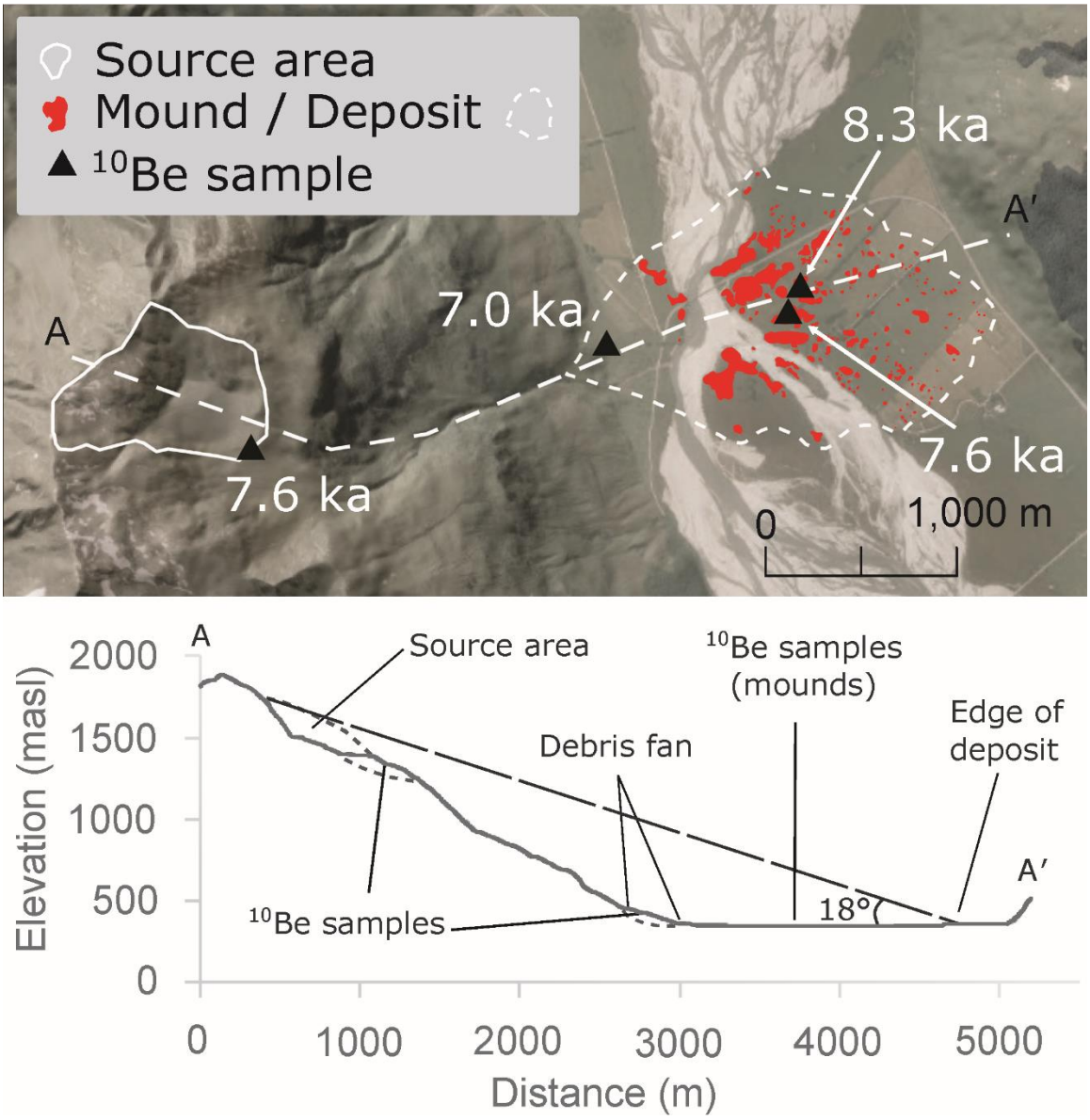

802

803 **Figure 8:** Map showing rock avalanche source area and deposit as mapped
804 in this study, with ^{10}Be exposure ages. Cross-section below is extracted from
805 LINZ 8 m DEM for the transect A-A′ shown on the map; the dashed lines
806 represent possible pre-failure topography. The travel angle of $\tan^{-1}$ (H/L) = 18° is
807 slightly higher than (the 14°) estimated using Coriminas' (1996) empirical
808 regression model, for a rockfall/avalanche volume of 22.5 M m^3, but it is within
809 the normal range for rock avalanches.